HHS Public Access

Author manuscript

Science. Author manuscript; available in PMC 2024 November 10.

Published in final edited form as:

Science. 2023 July 28; 381(6656): eadd6696. doi:10.1126/science.add6696.

TRIM11 protects against tauopathies and is downregulated in Alzheimer's disease

Zi-Yang Zhang[1,†], **Dilshan S. Harischandra**[1,†,‡], **Ruifang Wang**[1,†], **Shivani Ghaisas**[1,†,‡], **Janet Y. Zhao**[1,§], **Thomas P. McMonagle**[2,¶], **Guixin Zhu**[1,#], **Kenzo D. Lacuarta**[1], **Jianing Song**[1], **John Q. Trojanowski**[3], **Hong Xu**[3], **Virginia M.-Y. Lee**[3], **Xiaolu Yang**[1,*]

[1]Department of Cancer Biology and Abramson Family Cancer Research Institute, Perelman School of Medicine, University of Pennsylvania, Philadelphia, PA 19104

[2]College of Arts and Sciences, University of Pennsylvania, Philadelphia, PA 19104

[3]Department of Pathology and Laboratory Medicine, Institute on Aging, and Center for Neurodegenerative Disease Research, Perelman School of Medicine, University of Pennsylvania, Philadelphia, PA 19104

Abstract

Aggregation of tau into filamentous inclusions underlies Alzheimer's disease (AD) and numerous other neurodegenerative tauopathies. The pathogenesis of tauopathies remains unclear, which impedes the development of disease-modifying treatments. Here, by systematically analyzing human tripartite motif (TRIM) proteins, we identified a few TRIMs that could potently inhibit tau aggregation. Among them, TRIM11 was markedly down-regulated in AD brains. TRIM11 promoted the proteasomal degradation of mutant tau as well as superfluous normal tau. It also enhanced tau solubility by acting as both a molecular chaperone to prevent tau misfolding and a disaggregase to dissolve preformed tau fibrils. TRIM11 maintained the connectivity and viability of neurons. Intracranial delivery of TRIM11 through adeno-associated viruses ameliorated pathology, neuroinflammation, and cognitive impairments in multiple animal models of tauopathies. These results suggest that TRIM11 down-regulation contributes to the pathogenesis

*Correspondence: xyang@pennmedicine.upenn.edu.

‡Present address: Labcorp Early Development Laboratories Inc., Greenfield, IN 46140

§Present address: Department of Neurobiology, Northwestern University, Evanston, IL 60208

¶Present address: KPMG LLP, Philadelphia, PA 19103

#Present address: The Fourth Affiliated Hospital of Zhejiang University, Yiwu, Zhejiang, China

†These authors contributed equally to this work.

Author contributions: Z.-Y.Z. performed cell-free and cell culture experiments and analyzed human and mouse brain tissues. D.S.H. performed cell-free, cell culture, and animal experiments. R.W. screened TRIM proteins and performed cell-free and cell culture experiments. S.G. performed animal experiments. J.Z. performed IHC assay of mouse brain tissues and analyzed animal experiment results. T.P.M. performed animal experiments. G.Z. and J.S. helped with cell-free and cell culture experiments. K.D.L. helped with animal experiments. J.Q.T. provided human postmortem brain tissues. H.X., and V.M.-Y.L. provided human postmortem brain tissues, recombinant proteins, and cell lines, and advised on the analysis of human and animal tissues. V.M.-Y.L acquired funding. X.Y. conceived and supervised the study and acquired funding. X.Y., Z.-Y. Z., D.S.H., R.W., and S.G. designed the experiments. X.Y. prepared the manuscript with contributions from Z.-Y.Z., D.S.H., R.W., S.G., J.Z., and T.P.M., major inputs from V. M.-Y. L. and H.X., and comments from all other authors. T.P.M. participated in this work prior to joining KPMG; no official support or endorsement by KPMG is intended or inferred.

Competing interests: X.Y. is an inventor on a patent application owned by the University of Pennsylvania related to TRIM proteins, and a co-founder and equity holder of Evergreen Therapeutics LLC, which received investments from Wealth Strategy Holding Limited. The other authors declare no competing financial interests.

of tauopathies and that restoring TRIM11 expression may represent an effective therapeutic strategy.

One Sentence Summary

TRIM11 is downregulated in Alzheimer's disease, and restoring its expression may lead to effective therapies.

Intracellular neurofibrillary tangles (NFTs) composed of hyperphosphorylated forms of the microtubule-associated protein tau is the pathological hallmark shared by more than twenty heterogeneous dementias and movement disorders, collectively referred to as tauopathies (1–3). Among them, progressive supranuclear palsy (PSP), corticobasal degeneration, Pick's disease (PiD), and many others are primary tauopathies that display no other major pathological abnormalities, whereas Alzheimer's disease (AD), the most common cause of dementia, is a secondary tauopathy additionally characterized by the presence of extracellular amyloid β (Aβ) plaques (4, 5). In a familial subset of primary tauopathies, the tau-encoding gene *MAPT* is mutated (6–8). In both primary tauopathies and AD, NFT burden correlates with cognitive decline and neurodegeneration (9–11). Moreover, tau is required for Aβ-induced neurotoxicity (12). Therefore, tau misfolding and aggregation likely represent the main disease-causing event for AD and the other tauopathies.

To maintain proteins in their functional soluble form, organisms in all kingdoms of life have evolved protein quality control (PQC) systems (13–15). These systems include degradative pathways that recycle defective proteins and superfluous normal proteins, molecular chaperones that prevent protein misfolding and aggregation, and disaggregases that dissolve pre-existing protein deposits. The conversion of tau from soluble monomers to fibrillar aggregates in tauopathies in an age-dependent manner suggests a diminishing capacity of a PQC system that can normally protect against tau aggregation. Nevertheless, the identity and nature of such a PQC system remain undefined.

Tripartite motif (TRIM) proteins are defined by a TRIM/RBCC region consisting of a RING domain, one or two B-box motifs, and a coiled-coil region (fig. S1) (16, 17). These proteins are present only in metazoans and their number has expanded substantially during evolution, including over 70 in humans. Recent studies suggest that some TRIM proteins may participate in PQC (18–21), although other TRIMs can aggravate protein aggregation (22). Moreover, TRIM21, a cytoplasmic antibody receptor, mediates degradation of antibody-coated viruses or extracellular proteins that happen to enter the cytoplasm or intracellular proteins for which specific antibodies can be delivered (23–27). Here, we examine the role of the TRIM system in the pathogenesis of tauopathy, investigate its mechanism of action, and explore its utility for disease treatment.

Systematic analysis of TRIM proteins

To determine the effect of TRIM proteins on tau aggregation, we combined two approaches: (1) systematically analyzing virtually all known human TRIMs for their capability to remove tau aggregates in cultured cells, and (2) for TRIMs that exhibit a potent effect,

comparing their expression in postmortem brain tissues from AD and control individuals. For the systematic analysis, we cloned seventy-five TRIMs individually into a mammalian expression vector (Table S1). Each TRIM was introduced in HEK293T cells together with GFP-tau P301L, an enhanced green fluorescence protein (GFP) fusion of the longest isoform of human tau (441 residues with 2 N-terminal inserts and 4 microtubule binding repeats, 2N4R) carrying P301L, a mutation associated with familial tauopathies (6, 8). GFP-tau P301L alone generated aggregated species that were insoluble in non-ionic detergent (Fig. 1, A to C). When co-expressed with GFP-tau P301L, the majority of TRIMs were unable to clear GFP-tau P301L aggregates. However, three TRIMs (TRIM10, −11, and −55) displayed a robust effect, reducing GFP-tau P301L aggregates nearly completely, while two TRIMs (TRIM26 and −36) displayed a relatively moderate effect (Fig. 1, A to C).

To further examine the effect of these five TRIMs on tau, we used two neural cell lines, SH-SY5Y and Neuro-2a (N2a). TRIM10, −11, −36, and −55 strongly reduced GFP-tau P301L aggregates in both SH-SY5Y (Fig. 1, D and E, and fig. S2A) and N2a (fig. S2, B and C) cells. They also reduced GFP-tau P301L aggregates in N2a cells insoluble in the zwitterionic detergent sarkosyl (fig. S2, D and E), which likely contained filamentous tau (28). In contrast, TRIM26 showed minimal or moderate activity (Fig. 1, D and E, and fig. S2, A to E). With the exception of TRIM36 in HEK293T cells, none of these TRIMs reduced levels of *GFP-tau P301L* transcript in HEK293T, SH-SY5Y, or N2a cells (fig. S2, F to H).

Conversely, we knocked out each of these five TRIMs in HEK293T cells by means of CRISPR-mediated gene editing. Knockout of TRIM10, −11, or −55 increased GFP-tau P301L aggregates by ~80–130% without altering *GFP-tau P301L* mRNA levels, whereas knockout of TRIM36, as well as TRIM26, had no effect on GFP-tau P301L aggregates (Fig. 1, F and G, and fig. S3, A and B). We also knocked down these TRIMs in N2a cells by small interfering RNA (siRNA). Knockdown of TRIM10, −11, or −55 increased GFP-tau P301L aggregates by ~50–180% without affecting *GFP-tau P301L* mRNA, whereas knockdown of TRIM36 had no effect (Fig. 1, H and I, and fig. S3, C to H). For overexpression and knockout/knockdown, TRIM11 consistently displayed the strongest effect. Collectively, these results indicate that TRIM10, TRIM55, and especially TRIM11 possess potent activity to clear mutant tau.

Downregulation of TRIM11 in AD brains

To evaluate whether TRIM10, −11, or −55 might be downregulated in AD brains, we compared their RNA and protein levels in postmortem brain tissues from twenty-three sporadic AD individuals and fourteen age- and sex-matched control individuals with no known neurodegenerative diseases (Fig. 2A and Table S2). Tau pathology in the AD samples was verified by the reactivity to four antibodies that recognize abnormally phosphorylated tau (p-tau) species (Fig. 2B and fig. S4A), as well as the formation of high molecular weight tau species that were resistant to anionic detergent sodium dodecyl sulfate (SDS) (fig. S4B). Each of the *TRIM10*, *TRIM11*, and *TRIM55* transcripts was present at similar levels in AD and control tissues (fig. S4C). Levels of TRIM10 or TRIM55 protein were also comparable in these tissues (Fig. 2, B and C).

Interestingly, however, TRIM11 protein was present at a substantially lower level in AD compared to control tissues, with a ~55% reduction on average (Fig. 2, B and D, and fig. S4, D and E). This reduction was corroborated by immunohistochemistry (IHC) (Fig. 2, E and F), as well as by immunofluorescence (IF) controlled for the number of neurons (Fig. 2, G and H) or total neural cells (fig. S4, F and G). These observations, along with the comparable abundance of the *TRIM11* transcript in AD and control brains (fig. S4C) and the unmatched TRIM11 mRNA and protein levels in individual AD samples (fig. S4H), suggested that TRIM11 reduction in AD brains preceded neuronal loss.

Across control and AD brain tissues, there was a strong inverse correlation between TRIM11 expression and levels of each of the four p-tau species (Fig. 2I). Among the AD tissues, there was also an inverse correlation between TRIM11 expression and levels of two p-tau species (Fig. 2J), albeit not the others (fig. S4I). Together, these results indicate that TRIM11 is downregulated during sporadic AD pathogenesis with a strong association to tau pathology, and that the change in TRIM11 expression is probably due to a post-transcriptional mechanism. Of note, single nucleotide polymorphisms (SNPs) in the *TRIM11* gene are linked to rare cases of PSP, a prevalent form of sporadic tauopathy (29). Therefore, we focus on TRIM11 in the studies described below.

TRIM11 promotes tau degradation

The strong ability of TRIM11 to clear tau aggregates, as well as its downregulation in AD brains, prompted us to investigate its mechanism of action. We first evaluated whether TRIM11 targets tau for degradation, a possibility suggested by the screening of TRIMs (Fig. 1, and figs S2 and S3). Tau is a substrate of the ubiquitin-proteasome system (30, 31), while accumulation of insoluble tau impairs proteasome activity, further exacerbating tau pathology (32). The commitment to proteasomal degradation occurs at the level of substrate recognition; yet, how tau is specifically recognized for proteasomal degradation remains unclear.

Upon co-expression in HEK293T cells, TRIM11 reduced levels of GFP-tau P301L in a dose-dependent manner (Fig. 3A). A cycloheximide (CHX) chase assay showed that TRIM11 accelerated the turnover of aggregated GFP-tau P301L and prolonged its half-life (Fig. 3B and fig. S5A). To corroborate this observation, we introduced mCherry or mCherry plus TRIM11 in QBI293 cells that express tau P301L-GFP in a doxycycline (Dox)-inducible manner (QBI293/tau P301L-GFP cells) (33). Upon induction and then termination of tau P301L-GFP synthesis, the turnover of preexisting tau P301L-GFP and p-tau P301L-GFP was accelerated in TRIM11/mCherry-expressing cells compared to mCherry-expressing cells (Fig. 3C, and fig. S5B). Conversely, we knocked out endogenous TRIM11 and observed a slowdown in GFP-tau P301L degradation (fig. S5, C and D).

Treatment with the protein phosphatase inhibitor okadaic acid (OA) increased levels of p-tau species (34) (Fig. 3D and fig. S5E). TRIM11 reduced levels of OA-induced p-tau species and nearly completely cleared them in the insoluble fraction (Fig. 3D and fig. S5, F to I). TRIM11 also decreased levels of overexpressed wild-type tau (Fig. 3A) and accelerated its turnover (fig. S5, J and K), whereas knocking out TRIM11 by CRISPR-

mediated gene editing slowed turnover of overexpressed wild-type tau (fig. S5, L and M). TRIM11-mediated degradation of mutant and wild-type tau was prevented by the proteasome inhibitor MG132, but not the lysosome inhibitors leupeptin and ammonium chloride (NH_4Cl) in combination (LN) (fig. S6, A and B). Together, these results indicate that TRIM11 targets mutant and hyperphosphorylated tau, as well as superfluous normal tau, for proteasomal degradation.

TRIM11 binds to and SUMOylates tau

To evaluate whether TRIM11 interacts with tau, we performed a bimolecular fluorescence complementation (BiFC) assay based on the fluorescent protein Venus (35). We fused TRIM11 and tau to the N- and C-terminal fragments of Venus, respectively, generating TRIM11-VN and tau-VC (fig. S6C, left panel). When TRIM11-VN and tau-VC were expressed together, but not individually, fluorescence was detected (Fig. 3E and fig. S6D). We also generated TRIM11-VC and tau-VN (fig. S6C, middle panel) and again observed fluorescence only when these fusions were expressed together (fig. S6, E and F). Thus, TRIM11 and tau interacted in cells, bringing the VN and VC moieties into close proximity to reconstitute Venus.

The interaction between exogenous TRIM11 and tau in cells was also detected by a co-immunoprecipitation assay (Co-IP) (Fig. 3F and fig. S6G). This interaction was stronger upon treatment with OA (Fig. 3F), or when wild-type tau was replaced with tau P301L (fig. S6G) or tau AT8, a tau mutant (S199E/S202E/T205E) that mimics the AT8-reactive p-tau (fig. S6H). In a cell-free assay with purified recombinant proteins (fig. S6I), tau and especially tau P301L was pulled down by GST-TRIM11, but not GST (Fig. 3G), indicating that TRIM11 can directly bind to tau.

Endogenous TRIM11 and tau co-localized with each other in SH-SY5Y and N2a cells as shown by IF, and this co-localization was increased following OA treatment (Fig. 3, H and I, and fig. S7, A to C). They also interacted with each other in SH-SY5Y and N2a cells as shown by a proximity ligation assay (PLA); this interaction was again increased in OA-treated cells (Fig. 3, J and K, and fig. S7, D to F). While increasing tau phosphorylation, OA treatment also noticeably elevated TRIM11 protein and mRNA levels (fig. S7, G to J). Collectively, these results indicate that TRIM11 interacts with tau, preferentially mutant or hyper-phosphorylated species.

TRIM proteins possess SUMO E3 ligase activity (18, 21, 36). For the nucleus-localized TRIM19 (a.k.a. PML), this activity promotes conjugation of nuclear misfolded proteins to poly-SUMO2/3 chains, permitting ubiquitination of these misfolded proteins by SUMO-targeted ubiquitin ligases (STUbLs) and their subsequent degradation in the proteasome (18). TRIM11, like tau, is primarily a cytoplasmic protein (20, 21). TRIM11 increased SUMOylation of tau in cells, and this activity was more pronounced for tau P301L than for tau (fig. S8A). In a cell-free assay with purified recombinant proteins (fig. S6I), TRIM11 directly SUMOylated tau and especially the mutant form (Fig. 3L and fig. S8B). By contrast, $TRIM11^{2EA}$, in which the two conserved Glu residues proximal to the RING domain were replaced with Ala (21), exhibited no such activity (Fig. 3L). $TRIM11^{2EA}$ also failed

to promote tau degradation (Fig. 3M). Collectively, these results indicate that TRIM11 SUMOylates tau, promoting its degradation in the proteasome.

TRIM11 enhances tau solubility

While defective proteins and superfluous normal proteins are removed by degradative pathways, the vast majority of tauopathy cases are sporadic in which normal tau protein expressed at physiological levels forms fibrillar aggregates (4). To maintain protein solubility, cells employ molecular chaperones and disaggregases, which prevent and reverse protein aggregation, respectively (37–39). TRIM11 preferentially removed insoluble tau, hence increasing the fraction of tau molecules that was soluble (e.g., see fig. S9, A and B). This was the case even under conditions when the total amounts of tau protein were comparable in the presence or absence of TRIM11 (Figs 3D and 4A, and fig. S9C). TRIM11-mediated tau solubilization was evident when cells were treated with MG132 or NH_4Cl (Fig. 4A), indicating its independence of tau degradation. Moreover, under conditions where total GFP-tau P301L levels remained comparable, TRIM11 dramatically reduced the amount of abnormally phosphorylated GFP-tau P301L species in both soluble and insoluble fractions (fig. S9D).

Aggregation of tau occurs through a rate-limiting nucleation step that involves its self-association (40). To assess the effect of TRIM11 on tau self-association in cells, we performed a BiFC assay in which tau was fused to VN or VC (41) (fig. S6C, right panel). When tau-VN and tau-VC were expressed together, but not individually, fluorescence signal was produced, indicating tau self-association (Fig. 4, B and C). When present at low levels that did not alter tau abundance, TRIM11 noticeably reduced the fluorescence signal (Fig. 4, B and C). Conversely, knockdown of TRIM11 increased the fluorescence signal in cells expressing tau-VN and tau-VC (fig. S9, E and F). Knockout of TRIM11 had a similar effect (fig. S9, G and H). These results indicate that TRIM11 enhances tau solubility and prevents its self-association.

TRIM11 inhibits the seeding of tau aggregates

Tauopathies are characterized by focal formation of tau aggregates and their spread along interconnected neuronal regions (42–44). Reflecting this prion-like, self-templating propagation, preformed fibrils (PFFs) of tau can seed aggregation of intracellular soluble tau (45–48). To examine whether TRIM11 protects against PFFs-seeded tau fibrillization, we used HEK293 that stably express RD(LM)-YFP, in which the tau repeat domain (RD) harboring the pro-aggregation mutations P301L and V337M is fused to yellow fluorescence protein (YFP) (48). Treatment of the HEK293/RD(LM)-YFP cells with PFFs generated from recombinant tau protein induced aggregation of intracellular RD(LM)-YFP, as shown by the appearance of inclusions in cells (Fig. 4, D and E) and an increase in insoluble species in cell lysates (fig. S9, I and J). Forced expression of TRIM11 reduced PFFs-induced RD(LM)-YFP inclusions and aggregates, while having a minimal effect on levels of soluble RD(LM)-YFP (Fig. 4, E and F, and fig. S9, I and J).

In an alternative approach, we treated QBI293/tau P301L-GFP cells with PFFs to seed aggregation of intracellular tau P301L-GFP (Fig. 4, F to H). When introduced into these cells, TRIM11 strongly decreased both tau inclusions in cells (Fig. 4, F and G) and tau aggregates in cell lysates (Fig. 4H). Preceding the formation of fibrillar aggregates, tau, similar to other misfolding-prone proteins linked to neurodegeneration (49), assembles into soluble oligomeric species, which could be neurotoxic (50). Forced expression of TRIM11 also reduced formation of tau oligomers, as assayed with the tau oligomer-specific antibody T22 (51) (Fig. 4H). Therefore, TRIM11 protects against PFFs-seeded aggregation of intracellular tau into soluble oligomers and insoluble fibrils.

TRIM11 is a molecular chaperone for tau

The ability of TRIM11 to maintain tau solubility even in the face of PFFs prompted us to investigate whether TRIM11 can function as a molecular chaperone, a disaggregase, or both for tau. In the presence of heparin, recombinant tau protein spontaneously produced amyloid fibrils (52). This was indicated by a thioflavin T (ThT)-binding assay (Fig. 4I); western and dot blots that detected pelletable SDS-soluble (PE) and SDS-resistant (SR) aggregates, respectively (Fig. 4J); and electron microscopy (EM) that directly visualized mature tau fibrils (Fig. 4K). GST-TRIM11, but not GST, purified from bacterium (fig. S6I) effectively prevented tau fibrillization, reducing it by ~30% at a 1:80 molar ratio to tau and by ~60% at a 1:20 molar ratio (Fig. 4, I and J). EM analysis confirmed that TRIM11 blocked the formation of mature tau fibrils (Fig. 4K). Moreover, TRIM11 prevented aggregation of tau P301L into amyloid fibrils and other high molecular weight species (Fig. 4, L and M). TRIM11 also effectively blocked fibrillization GST-tau (fig. S10, A to C). At a molar ratio of 1:20, TRIM11 almost completely blocked the formation of GST-tau fibrils (fig. S10A). These observations indicate that TRIM11 is a potent molecular chaperone for tau, preventing its misfolding and aggregation. Distinctive from canonical chaperones such as the HSP70 and HSP90 systems, which are multicomponent machineries driven by energy derived from ATP hydrolysis (15), TRIM11 obviates tau aggregation on its own, in the absence of any other protein components or ATP (Fig. 4, I to M, and fig. S10, A to C).

TRIM11 is a disaggregase for tau

Amyloid fibrils, which comprise of β strands that stack perpendicularly to the fibril axis (cross-β structure), are highly organized, energetically stable structures (53, 54). Their dissolution usually requires coordinated action of multiple factors in an ATP-dependent manner (39, 55). Bacterial, fungal, and plant cells contain a disaggregation system comprised of HSP70, its co-chaperone HSP40, and the AAA^+-ATPase HSP104 (56), but this system is absent in metazoans. Recent studies showed that mammalian HSP70/HSP40 and HSP110 (an atypical HSP70 family) can work together as a disaggregase (57–59). Yet, this disaggregation system fragments amyloid fibrils, generating small seeds that promote, rather than suppressing, aggregation of tau and other misfolding-prone proteins and hence exacerbating their neurotoxicity (60, 61).

When incubated with tau fibrils, TRIM11 was capable of dissolving these aggregates, reducing their bindings to ThT (Fig. 4N) and converting the majority of them to a soluble

state (Fig. 4O). This activity was verified by EM analysis (Fig. 4P). Similarly, TRIM11 could dissolve GST-tau fibrils (fig. S10, D and E). Thus, TRIM11 is also a disaggregase for tau. As for its molecular chaperone activity, TRIM11 dissolved pre-existing tau fibrils on its own. Importantly, unlike the mammalian HSP70/HSP40-HSP110 system, TRIM11 effectively abrogates the formation and seeding of tau aggregates in cells (Fig. 4, A to H, and fig. S9).

TRIM11 protects primary neurons against tau aggregation

In primary neurons derived from wild-type mice, as in neural cell lines, endogenous TRIM11 and tau co-localized with each other (Fig. 5A and fig. S11, A and B). They also interacted with each other in primary neurons, as shown by a PLA assay (fig. S11, C and D). Treatment with OA, which elevated TRIM11 levels (fig. S11, E and F), augmented the TRIM11-tau interaction (fig. S11, C and D). Moreover, TRIM11 interacted with AT8-reactive p-tau in human brain tissues, and this interaction was much stronger in AD compared to control tissues (fig. S11, G and H).

To assess the effect of TRIM11 downregulation on tau aggregation, we generated several antisense oligonucleotides (ASOs) comprised of 2′-deoxy-2′fluoro-D-arabinonucleic acid (FANA) (62) against *Trim11*. These FANA-ASOs effectively entered cultured neurons and silenced *TRIM11* expression to different extents (fig. S12, A and B). We treated cortical neurons derived from PS19 transgenic mice that express human tau P301S (63), with PFFs formed by myc-K18/P301L, a truncated tau protein consisting of the microtubule-binding domain with the P301L mutation (47). This led to the formation of neuritic thread-like inclusions reactive to AT8 and MC1 (Fig. 5, B and C, and fig. S12, C and D), the latter recognizing a disease-specific conformation of tau. Silencing *Trim11* by FANA-ASO exacerbated tau aggregation, increasing AT8- and MC1-reactive tau by ~50–90% (Fig. 5, B and C, and fig. S12, C and D).

To evaluate the effect of TRIM11 upregulation, we cloned TRIM11 and, as a control, GFP into the adeno-associated virus AAV9 vector, a serotype that effectively targets cells in the central nervous system (64) (fig. S12E). When treated with myc-K18/P301L PFFs, AAV9-TRIM11-transduced PS19 cortical neurons exhibited a ~60% reduction in AT8- and MC1-reactive tau compared to AAV9-GFP-transduced neurons (Fig. 5, D and E, and fig. 11, F and G). Likewise, when hippocampal neurons derived from PS19 mice were treated with myc-K18/P301L PFFs, substantially less AT8- and MC1-reactive tau appeared in AAV9-TRIM11-tranduced neurons than in AAV9-GFP-transduced neurons (fig. S12, H and I). These results indicate that TRIM11 affords neurons protection against tau aggregation.

TRIM11 maintains neuronal viability and connectivity

Synaptic degeneration is a prominent feature of AD patients and mouse models, proceeding neuronal loss and correlating strongly with cognitive decline (65). To evaluate the role of TRIM11 in synapse formation, we probed neurons with antibodies to the presynaptic marker synaptophysin (SYP) and postsynaptic density protein 95 (PSD95). Silencing TRIM11 in wild-type cortical neurons by ASOs led to a reduction in SYP-positive puncta (by ~40%;

Fig. 5, F and G) and PSD95-positve puncta (by ~30%; Fig. 5, H and I), as well as their juxtaposition (Fig. S12, J and K). TRIM11-depleted neurons also contained lower levels of neurofilament light chain (NFL) (~40% reduction), a component of the axonal scaffold, but not microtubule-associated protein 2 (MAP2), which stabilizes microtubules in the dendrites (Fig. 5, J to L, and Fig. S12L). Moreover, silencing TRIM11 with various ASOs reduced the viability of cortical neurons in a manner that was correlated with the effect of these ASOs on *TRIM11* expression (Fig. 5M and fig. S12B). These results suggest that endogenous TRIM11 is a neuroprotective factor, and its downregulation impairs neuronal viability and connectivity.

Conversely, forced TRIM11 expression via AAV9-mediated transduction increased SYP- and PSD95-positive puncta by ~70% and ~50%, respectively (Fig. 5, N to Q). TRIM11 also elevated expression of NFL (by ~50%), but not MAP2 (Fig. 5, R to T). Moreover, TRIM11 conferred neurons resistance to tau PFF-induced cytotoxicity (Fig. 5U). Therefore, TRIM11 upregulation enhances neuronal integrity and synaptic formation.

TRIM11 ameliorates tau pathology, neuroinflammation, and cognitive impairments in PS19 mice

Next, we evaluated the protective effect of TRIM11 in mouse models of tauopathy. We first used PS19 transgenic mice, a widely-utilized tauopathy model that progressively accumulates tau inclusions, resembling human AD and other tauopathy patients (63). AAV9-TRIM11 or AAV9-GFP vector was delivered to the hippocampus of these mice via bilateral stereotaxic injection at 2.5 months of age, and brain pathology and animal behaviors were analyzed at ~10 months of age (Fig. 6A). As expected, hippocampi of AAV9-GFP-injected mice displayed strong NFT-like tau inclusions in various regions (Fig. 6B and Fig. S13A). In comparison, hippocampi of AAV9-TRIM11-injected mice contained substantially less tau pathology (~55% reduction) (Fig. 6B and Fig. S13A). This reduction was corroborated by immunoblot analysis, which showed that TRIM11 strongly reduced insoluble and soluble p-tau species (Fig. 6C, and Fig. S13, B to D). The inhibitory effect of TRIM11 was dose-dependent, as hippocampi with higher TRIM11 expression contained less p-tau species (Fig. 6C).

Astrogliosis parallels the distribution and density of NFTs in tauopathies (66, 67), and is an early pathological manifestation of PS19 mice (63). AAV9-GFP-injected brains displayed strong staining of glial fibrillary acidic protein (GFAP) (Fig. 6, D and E, and Fig. S13E), indicative of astrocyte activation. In comparison, AAV9-TRIM11-injected brains exhibited a ~50% reduction in GFAP immunoreactivity, to a level that was observed in un-injected brains of age-matched wild-type littermates (Fig. 6, D and E, and Fig. S13E). Activation of microglia was also detected in AAV9-GFP-injected brains, as shown by increased immunoreactivity to ionized calcium-binding adaptor molecule 1 (Iba1) (Fig. 6, F and G, and Fig. S13F). By contrast, AAV9-TRIM11-injected brains showed a ~40% reduction of microgliosis, again to a level seen in wild-type brains (Fig. 6, F and G, and Fig. S13F).

Similar to human tauopathies, tau dysfunction in PS19 mice is associated with neuronal loss, especially in hippocampi (63). Compared to hippocampi of the GFP group of

animals, hippocampi of the TRIM11 group of animals exhibited a ~50% increase in immunoreactivity for MAP2 (Fig. 6, H and I, and Fig. S13G). They also showed a ~70% increase in immunoreactivity for NFL, to a level comparable to that in hippocampi of the wild-type group of animals (Fig. 6, J and K, and Fig. S13H). Moreover, hippocampi of AAV9-TRIM11-treated animals displayed an ~40% increase in the expression of NeuN (Fig. 6, L and M, and Fig. S13I). These results indicate that TRIM11 rescues axonal and dendritic degeneration and neuronal loss in PS19 mice.

AD and many other tauopathies are characterized by a progressive decline in cognitive function (4, 5). To evaluate learning and memory ability, we performed an object recognition test (ORT) in which the propensity of mice to examine a novel object was observed (68). The GFP group of mice showed no difference in the times interacting with familiar and novel objects (i.e., ~50% preference to each). In contrast, the TRIM11 group of mice exhibited a ~77% preference to the novel subject, similar to that of wild-type mice (Fig. 6N), suggesting that TRIM11 rescues the deterioration of the long-term memory. Decline in motor strength is another tau-dependent defect in PS19 mice (69). In a wire hang test, the TRIM11 group of mice exhibited a substantially longer latency to fall (~75 sec) compared to the GFP group of mice (~50 sec), albeit they were still weaker than wild-type mice (Fig. 6O). Collectively, these results indicate that intracranial delivery of AAV9-TRIM11 in PS19 mice prevents tau pathology, neurodegeneration, and gliosis, and that it also improves cognitive and motor functions.

TRIM11 prevents PFFs-accelerated disease phenotypes in PS19 mice

Inoculation of tau PFFs into brains of PS19 mice before the onset of tauopathy induces focal formation and widespread transmission of tau aggregates, accelerating neuroinflammation and cognitive and motor deterioration (47). To evaluate whether TRIM11 protects against PFFs-accelerated disease phenotypes, we inoculated PFFs generated from recombinant myc-K18/P301L (47), together with either AAV9-TRIM11 or AAV9-GFP, unilaterally into the hippocampus of PS19 mice at 8 weeks of age and analyzed disease phenotypes at 12 weeks of age (Fig. 7A). When co-inoculated with AAV9-GFP, myc-K18/P301L PFFs induced a substantially amount of tau aggregates in the ipsilateral hippocampus (Fig. 7B and Fig. S14A). In comparison, when co-inoculated with AAV9-TRIM11, myc-K18/P301L induced ~45% less tau aggregates (Fig. 7B and Fig. S14A). Levels of abnormally phosphorylated tau were also noticeably declined in both soluble and insoluble fractions in AAV9-TRIM11-coinjected brains (Fig. 7C and Fig. S14, B to D). In the presence of AAV9-GFP, myc-K18/P301L PFFs elicited astrogliosis and microgliosis. In contrast, however, in the presence of AAV9-TRIM11, numbers of reactive astrocytes and microglia did not increase above those seen in wild-type mouse brains (Fig. 7, D and E, and Fig. S14, E and F).

In an ORT, the TRIM11 group of animals showed a preference to the novel subject that was comparable to that of wild-type animals, whereas the GFP group of animals showed no such preference (Fig. 7F). Therefore, TRIM11 obviated the decline in long-term memory. To assess the effect of TRIM11 on short-term memory, we measured spontaneous alternation behavior (SAB) in the Y-maze (70). The TRIM11 group exhibited significantly more spontaneous alternations (~56%) than the GFP group (~35%), reaching a level shown by

wild-type mice (Fig. 7G). Thus, TRIM11 also prevented the decline in the hippocampus-dependent working memory.

To evaluate motor function and anxiety-like phenotypes, we performed an open field test. Compared to the GFP group of mice, the TRIM11 group of mice travelled a longer distance (~36% increase) (Fig. 7, H and I) and stopped for a shorter period of time (~40% reduction) (Fig. 7J). These behaviors of TRIM11 mice were again similar to those of wild-type mice (Fig. 7, H to J). Together, these results indicate that TRIM11 inhibited the seeding and cell-to-cell transmission of tau aggregates in PS19 mice, preventing the activation of glial cells and the decline in cognitive and motor abilities.

TRIM11 ameliorates tau pathology and cognitive defects in 3×Tg-AD mice

In addition to tau-containing intraneuronal NFTs, AD is characterized by extracellular plaques comprised of Aβ peptide (4, 5). To evaluate the protective effect of TRIM11 on the combined pathological effects of tau and Aβ, we used a triple transgenic AD model (3×Tg-AD), which expresses tau P301L as well as familial mutations in two AD-related proteins, the amyloid precursor protein (APP) K595N/M596L (the Swedish mutation) and the presenilin 1 (PS1) M146V (71). 3×Tg-AD mice demonstrate both Aβ plaque and tau tangles, resembling human AD. We delivered AAV9-TRIM11 or AAV9-GFP to the hippocampus of 3×Tg-AD mice at 12 months of age, when they already showed a substantial amount of tau pathology in this brain region, and performed pathology and behavior analysis one month later (Fig. 8A). Delivery of AAV9-TRIM11 led to a substantial reduction in tau pathology compared to that of AAV9-GFP, as shown by IHC analysis (~30% reduction) (Fig. 8B and Fig. S15A). This reduction was corroborated by western blot analysis, which indicated a ~80–90% reduction in p-tau species reactive to AT8 and PHF-1 (Fig. 8C, and Fig. S15, B to D). Levels of AT8 staining in AAV9-TRIM11-injected brains at 13 months of age were lower than those in un-injected brains at 12 months of age (Fig. S15A), suggesting that TRIM11 cleared pre-existing tau aggregates. GFAP and Iba1 immunoreactivity was also markedly lower in the hippocampus of AAV9-TRIM11-injected animals compared to that in AAV9-GFP-injected animals, being reduced by ~30% and 60%, respectively (Fig. 8, D to G, and Fig. S15, E and F).

In 3×Tg-AD mice, cognitive impairment initially manifests at 4 months of age and progresses as tau tangles and Aβ plaques accumulate (71). Compared to AAV9-GFP-injected animals, AAV9-TRIM11-injected animals spent significantly more time exploring the novel object and less time on the familiar object in the ORT (Fig. 8H). They also spent more time exploring different arms in the Y-maze test (Fig. 8I). Moreover, the TRIM11 group of animals exhibited higher locomotive activity in an open filed test, traveling longer distance and stopping for less time (Fig. 8, J and K). Therefore, TRIM11 suppressed tau pathology and neuroinflammation and improves cognitive and motor ability of 3×Tg-AD mice.

Effect of CSF delivery of TRIM11

The animal experiments described above not only demonstrated the role of TRIM11 in protecting against tau-dependent neurodegeneration in mammalian brains, but also suggested a potential utility of the *TRIM11* gene in disease treatment. However, the intraparenchymal (IP) infusion used in these experiments was spatially restricted, whereas AD and many other tauopathies affect multiple brain regions. Thus, we investigated the effect of administering AAV vectors globally in the brain via the cerebrospinal fluid (CSF). We delivered AAV9-TRIM11 and AAV9-GFP by intracerebroventricular (ICV) injection to 3×Tg-AD mice at 9 months of age and analyzed mouse behaviors and pathology one to four months later (Fig. 8L). Compared to the GFP group of mice, the TRIM11 group of mice showed a ~35% reduction in tau-containing, NFT-like inclusions in the hippocampus (Fig. 8M) and a ~50–70% reduction in soluble and insoluble p-tau species in cell lysates (Fig. 8N and Fig. S16, A to C). The TRIM11 group of mice also showed a substantial reduction in GFAP- and Iba1-immunoreactivity, to levels that were close to, or only moderately higher than, those in the wild-type mice (Fig. 8, O and P, and Fig. S16, D and E). Moreover, compared to the GFP group of animals, the TRIM11 group of animals performed significantly better in the ORT and Y-maze tests (Fig. 8, Q and R) and showed higher locomotive ability in the open field test (Fig. 8S). These results suggest that CSF administration of the AAV9-TRIM11 vector might be beneficial for treating tauopathies.

Outlook

The current study reveals that TRIM11 plays a critical role in maintaining tau in its functional soluble state. TRIM11 achieves this important outcome through multiple mechanisms. It promotes proteasomal degradation of mutant and hyperphosphorylated tau as well as excess normal tau, thereby acting as a crucial link between tau and the proteasome. TRIM11 also serves as a molecular chaperone, preventing tau misfolding and aggregation. Moreover, TRIM11 functions as a disaggregase to dissolve preexisting tau deposits, including tau amyloid fibrils that are often intractable. Canonical PQC systems such as HSP60, HSP70, and HSP90 – which are conserved in both prokaryotes and eukaryotes – rely on coordinated actions of multiple components in an ATP-dependent manner. By contrast, TRIM11 can prevent and reverse tau aggregation by itself and independent of ATP. These multiple and potent activities of TRIM11 in combination are highly effective in protecting against tau misfolding and aggregation in various cell and animal models of tauopathy. The survey of virtually all human TRIMs shows that these activities of TRIM11 are likely shared by at least some other members of this large family. TRIM proteins, which are only identified in metazoans, might have evolved later during evolution in part to maintain the quality of the complex proteomes that enable these intricate life forms.

The downregulation of TRIM11 among sporadic AD brains, combined with its potent protective effect on tau, suggest that the diminished capacity of TRIM11 might contribute to tau aggregation and the associated pathological and cognitive changes. AD and other neurodegenerative tauopathies are becoming increasingly prevalent as the population ages, yet remain incurable. Tau, whose abnormality is both more closely linked to the disease progression than that of Aβ and required for the cytotoxicity of Aβ, represents a key

target for AD in addition to primary tauopathies (72). In recent years, gene therapy is becoming an important approach to treat neurological diseases (73). AAVs can transduce the non-dividing neurons and permit permanent expression of the therapeutic gene after a single administration (73, 74), with positive clinical outcomes (75). The effect of intraparenchymal and intraventricular delivery of AAV9-TRIM11 in animal models provides a proof of concept for the potential utility of the *TRIM11* gene to restore protein homeostasis in AD and other tauopathies, hence addressing the root cause of these devastating diseases.

Supplementary Material

Refer to Web version on PubMed Central for supplementary material.

Acknowledgement

We thank M. Diamond for providing cell lines, P. Davies for providing antibodies, and R. Wang, P. Zhang, and W. Prall for technical assistance.

Funding: This work was supported by a Sponsored Research Agreement grant from Wealth Strategy Holding Limited and an NIH grant (R01CA243520) to X.Y. and a pilot grant from Penn Institute for Translational Medicine and Therapeutics (under NIH grant UL1TR000003) to X.Y. and V.M.-Y.L.

Data and materials availability:

All data are available in the manuscript or the supplementary material. Requests for materials should be addressed to X.Y.

References and Notes:

1. Lee VM, Goedert M, Trojanowski JQ, Neurodegenerative tauopathies. Annu Rev Neurosci 24, 1121–1159 (2001). [PubMed: 11520930]
2. Spillantini MG, Goedert M, Tau pathology and neurodegeneration. Lancet Neurol 12, 609–622 (2013). [PubMed: 23684085]
3. Gotz J, Halliday G, Nisbet RM, Molecular Pathogenesis of the Tauopathies. Annu Rev Pathol 14, 239–261 (2019). [PubMed: 30355155]
4. Masters CL et al. , Alzheimer's disease. Nat Rev Dis Primers 1, 15056 (2015). [PubMed: 27188934]
5. Knopman DS et al. , Alzheimer disease. Nat Rev Dis Primers 7, 33 (2021). [PubMed: 33986301]
6. Hutton M et al. , Association of missense and 5'-splice-site mutations in tau with the inherited dementia FTDP-17. Nature 393, 702–705 (1998). [PubMed: 9641683]
7. Spillantini MG et al. , Mutation in the tau gene in familial multiple system tauopathy with presenile dementia. Proc Natl Acad Sci U S A 95, 7737–7741 (1998). [PubMed: 9636220]
8. Dumanchin C et al. , Segregation of a missense mutation in the microtubule-associated protein tau gene with familial frontotemporal dementia and parkinsonism. Hum Mol Genet 7, 1825–1829 (1998). [PubMed: 9736786]
9. Arriagada PV, Growdon JH, Hedley-Whyte ET, Hyman BT, Neurofibrillary tangles but not senile plaques parallel duration and severity of Alzheimer's disease. Neurology 42, 631–639 (1992). [PubMed: 1549228]
10. Ling H et al. , Characteristics of progressive supranuclear palsy presenting with corticobasal syndrome: a cortical variant. Neuropathol Appl Neurobiol 40, 149–163 (2014). [PubMed: 23432126]
11. Kouri N et al. , Neuropathological features of corticobasal degeneration presenting as corticobasal syndrome or Richardson syndrome. Brain 134, 3264–3275 (2011). [PubMed: 21933807]

12. Roberson ED et al. , Reducing endogenous tau ameliorates amyloid beta-induced deficits in an Alzheimer's disease mouse model. Science 316, 750–754 (2007). [PubMed: 17478722]
13. Balch WE, Morimoto RI, Dillin A, Kelly JW, Adapting proteostasis for disease intervention. Science 319, 916–919 (2008). [PubMed: 18276881]
14. Wolff S, Weissman JS, Dillin A, Differential scales of protein quality control. Cell 157, 52–64 (2014). [PubMed: 24679526]
15. Balchin D, Hayer-Hartl M, Hartl FU, In vivo aspects of protein folding and quality control. Science 353, aac4354 (2016). [PubMed: 27365453]
16. Hatakeyama S, TRIM proteins and cancer. Nat Rev Cancer 11, 792–804 (2011). [PubMed: 21979307]
17. Ozato K, Shin DM, Chang TH, Morse HC 3rd, TRIM family proteins and their emerging roles in innate immunity. Nat Rev Immunol 8, 849–860 (2008). [PubMed: 18836477]
18. Guo L et al. , A cellular system that degrades misfolded proteins and protects against neurodegeneration. Mol Cell 55, 15–30 (2014). [PubMed: 24882209]
19. Chen L et al. , Enhanced degradation of misfolded proteins promotes tumorigenesis. Cell Rep 18, 3143–3154 (2017). [PubMed: 28355566]
20. Chen L, Zhu G, Johns EM, Yang X, TRIM11 activates the proteasome and promotes overall protein degradation by regulating USP14. Nat Commun 9, 1223 (2018). [PubMed: 29581427]
21. Zhu G et al. , TRIM11 Prevents and Reverses Protein Aggregation and Rescues a Mouse Model of Parkinson's Disease. Cell Rep 33, 108418 (2020). [PubMed: 33264628]
22. Rousseaux MW et al. , TRIM28 regulates the nuclear accumulation and toxicity of both alpha-synuclein and tau. Elife 5, (2016).
23. Mallery DL et al. , Antibodies mediate intracellular immunity through tripartite motif-containing 21 (TRIM21). Proc Natl Acad Sci U S A 107, 19985–19990 (2010). [PubMed: 21045130]
24. Kondo A et al. , Antibody against early driver of neurodegeneration cis P-tau blocks brain injury and tauopathy. Nature 523, 431–436 (2015). [PubMed: 26176913]
25. Clift D et al. , A Method for the Acute and Rapid Degradation of Endogenous Proteins. Cell 171, 1692–1706 e1618 (2017). [PubMed: 29153837]
26. McEwan WA et al. , Cytosolic Fc receptor TRIM21 inhibits seeded tau aggregation. Proc Natl Acad Sci U S A 114, 574–579 (2017). [PubMed: 28049840]
27. Mukadam AS et al. , Cytosolic antibody receptor TRIM21 is required for effective tau immunotherapy in mouse models. Science 379, 1336–1341 (2023). [PubMed: 36996217]
28. Greenberg SG, Davies P, A preparation of Alzheimer paired helical filaments that displays distinct tau proteins by polyacrylamide gel electrophoresis. Proc Natl Acad Sci U S A 87, 5827–5831 (1990). [PubMed: 2116006]
29. Jabbari E et al. , Variation at the TRIM11 locus modifies progressive supranuclear palsy phenotype. Ann Neurol 84, 485–496 (2018). [PubMed: 30066433]
30. Chesser AS, Pritchard SM, Johnson GV, Tau clearance mechanisms and their possible role in the pathogenesis of Alzheimer disease. Front Neurol 4, 122 (2013). [PubMed: 24027553]
31. Lee MJ, Lee JH, Rubinsztein DC, Tau degradation: the ubiquitin-proteasome system versus the autophagy-lysosome system. Prog Neurobiol 105, 49–59 (2013). [PubMed: 23528736]
32. Myeku N et al. , Tau-driven 26S proteasome impairment and cognitive dysfunction can be prevented early in disease by activating cAMP-PKA signaling. Nat Med 22, 46–53 (2016). [PubMed: 26692334]
33. Guo JL et al. , The Dynamics and Turnover of Tau Aggregates in Cultured Cells: INSIGHTS INTO THERAPIES FOR TAUOPATHIES. J Biol Chem 291, 13175–13193 (2016). [PubMed: 27129267]
34. Gong CX et al. , Phosphorylation of microtubule-associated protein tau is regulated by protein phosphatase 2A in mammalian brain. Implications for neurofibrillary degeneration in Alzheimer's disease. J Biol Chem 275, 5535–5544 (2000). [PubMed: 10681533]
35. Shyu YJ, Liu H, Deng X, Hu CD, Identification of new fluorescent protein fragments for bimolecular fluorescence complementation analysis under physiological conditions. Biotechniques 40, 61–66 (2006). [PubMed: 16454041]

36. Chu Y, Yang X, SUMO E3 ligase activity of TRIM proteins. Oncogene 30, 1108–1116 (2011). [PubMed: 20972456]
37. Tyedmers J, Mogk A, Bukau B, Cellular strategies for controlling protein aggregation. Nat Rev Mol Cell Biol 11, 777–788 (2010). [PubMed: 20944667]
38. Hartl FU, Bracher A, Hayer-Hartl M, Molecular chaperones in protein folding and proteostasis. Nature 475, 324–332 (2011). [PubMed: 21776078]
39. Saibil H, Chaperone machines for protein folding, unfolding and disaggregation. Nat Rev Mol Cell Biol 14, 630–642 (2013). [PubMed: 24026055]
40. Friedhoff P, von Bergen M, Mandelkow EM, Davies P, Mandelkow E, A nucleated assembly mechanism of Alzheimer paired helical filaments. Proc Natl Acad Sci U S A 95, 15712–15717 (1998). [PubMed: 9861035]
41. Tak H et al. , Bimolecular fluorescence complementation; lighting-up tau-tau interaction in living cells. PLoS One 8, e81682 (2013). [PubMed: 24312574]
42. Jucker M, Walker LC, Self-propagation of pathogenic protein aggregates in neurodegenerative diseases. Nature 501, 45–51 (2013). [PubMed: 24005412]
43. Brettschneider J, Del Tredici K, Lee VM, Trojanowski JQ, Spreading of pathology in neurodegenerative diseases: a focus on human studies. Nat Rev Neurosci 16, 109–120 (2015). [PubMed: 25588378]
44. Frost B, Diamond MI, Prion-like mechanisms in neurodegenerative diseases. Nat Rev Neurosci 11, 155–159 (2010). [PubMed: 20029438]
45. Frost B, Jacks RL, Diamond MI, Propagation of tau misfolding from the outside to the inside of a cell. J Biol Chem 284, 12845–12852 (2009). [PubMed: 19282288]
46. Guo JL, Lee VM, Seeding of normal Tau by pathological Tau conformers drives pathogenesis of Alzheimer-like tangles. J Biol Chem 286, 15317–15331 (2011). [PubMed: 21372138]
47. Iba M et al. , Synthetic tau fibrils mediate transmission of neurofibrillary tangles in a transgenic mouse model of Alzheimer's-like tauopathy. J Neurosci 33, 1024–1037 (2013). [PubMed: 23325240]
48. Sanders DW et al. , Distinct tau prion strains propagate in cells and mice and define different tauopathies. Neuron 82, 1271–1288 (2014). [PubMed: 24857020]
49. Kayed R et al. , Common structure of soluble amyloid oligomers implies common mechanism of pathogenesis. Science 300, 486–489 (2003). [PubMed: 12702875]
50. Lasagna-Reeves CA et al. , Tau oligomers impair memory and induce synaptic and mitochondrial dysfunction in wild-type mice. Mol Neurodegener 6, 39 (2011). [PubMed: 21645391]
51. Lasagna-Reeves CA et al. , Identification of oligomers at early stages of tau aggregation in Alzheimer's disease. FASEB J 26, 1946–1959 (2012). [PubMed: 22253473]
52. Goedert M et al. , Assembly of microtubule-associated protein tau into Alzheimer-like filaments induced by sulphated glycosaminoglycans. Nature 383, 550–553 (1996). [PubMed: 8849730]
53. Eisenberg D, Jucker M, The amyloid state of proteins in human diseases. Cell 148, 1188–1203 (2012). [PubMed: 22424229]
54. Knowles TP, Vendruscolo M, Dobson CM, The amyloid state and its association with protein misfolding diseases. Nat Rev Mol Cell Biol 15, 384–396 (2014). [PubMed: 24854788]
55. Doyle SM, Genest O, Wickner S, Protein rescue from aggregates by powerful molecular chaperone machines. Nat Rev Mol Cell Biol 14, 617–629 (2013). [PubMed: 24061228]
56. Glover JR, Lindquist S, Hsp104, Hsp70, and Hsp40: a novel chaperone system that rescues previously aggregated proteins. Cell 94, 73–82 (1998). [PubMed: 9674429]
57. Shorter J, The mammalian disaggregase machinery: Hsp110 synergizes with Hsp70 and Hsp40 to catalyze protein disaggregation and reactivation in a cell-free system. PLoS One 6, e26319 (2011). [PubMed: 22022600]
58. Gao X et al. , Human Hsp70 Disaggregase Reverses Parkinson's-Linked alpha-Synuclein Amyloid Fibrils. Mol Cell 59, 781–793 (2015). [PubMed: 26300264]
59. Nillegoda NB et al. , Crucial HSP70 co-chaperone complex unlocks metazoan protein disaggregation. Nature 524, 247–251 (2015). [PubMed: 26245380]

60. Tittelmeier J et al. , The HSP110/HSP70 disaggregation system generates spreading-competent toxic alpha-synuclein species. EMBO J 39, e103954 (2020). [PubMed: 32449565]
61. Nachman E et al. , Disassembly of Tau fibrils by the human Hsp70 disaggregation machinery generates small seeding-competent species. J Biol Chem 295, 9676–9690 (2020). [PubMed: 32467226]
62. Kalota A et al. , 2'-deoxy-2'-fluoro-beta-D-arabinonucleic acid (2'F-ANA) modified oligonucleotides (ON) effect highly efficient, and persistent, gene silencing. Nucleic Acids Res 34, 451–461 (2006). [PubMed: 16421272]
63. Yoshiyama Y et al. , Synapse loss and microglial activation precede tangles in a P301S tauopathy mouse model. Neuron 53, 337–351 (2007). [PubMed: 17270732]
64. Foust KD et al. , Intravascular AAV9 preferentially targets neonatal neurons and adult astrocytes. Nat Biotechnol 27, 59–65 (2009). [PubMed: 19098898]
65. Spires-Jones TL, Hyman BT, The intersection of amyloid beta and tau at synapses in Alzheimer's disease. Neuron 82, 756–771 (2014). [PubMed: 24853936]
66. Muramori F, Kobayashi K, Nakamura I, A quantitative study of neurofibrillary tangles, senile plaques and astrocytes in the hippocampal subdivisions and entorhinal cortex in Alzheimer's disease, normal controls and non-Alzheimer neuropsychiatric diseases. Psychiatry Clin Neurosci 52, 593–599 (1998). [PubMed: 9895207]
67. Togo T, Dickson DW, Tau accumulation in astrocytes in progressive supranuclear palsy is a degenerative rather than a reactive process. Acta Neuropathol 104, 398–402 (2002). [PubMed: 12200627]
68. Lueptow LM, Novel Object Recognition Test for the Investigation of Learning and Memory in Mice. J Vis Exp, (2017).
69. Patel H et al. , Pathological tau and reactive astrogliosis are associated with distinct functional deficits in a mouse model of tauopathy. Neurobiol Aging 109, 52–63 (2022). [PubMed: 34655981]
70. Kraeuter AK, Guest PC, Sarnyai Z, The Y-Maze for Assessment of Spatial Working and Reference Memory in Mice. Methods Mol Biol 1916, 105–111 (2019). [PubMed: 30535688]
71. Oddo S et al. , Triple-transgenic model of Alzheimer's disease with plaques and tangles: intracellular Abeta and synaptic dysfunction. Neuron 39, 409–421 (2003). [PubMed: 12895417]
72. Li C, Gotz J, Tau-based therapies in neurodegeneration: opportunities and challenges. Nat Rev Drug Discov 16, 863–883 (2017). [PubMed: 28983098]
73. Deverman BE, Ravina BM, Bankiewicz KS, Paul SM, Sah DWY, Gene therapy for neurological disorders: progress and prospects. Nat Rev Drug Discov 17, 641–659 (2018). [PubMed: 30093643]
74. Naldini L, Gene therapy returns to centre stage. Nature 526, 351–360 (2015). [PubMed: 26469046]
75. Mendell JR et al. , Single-Dose Gene-Replacement Therapy for Spinal Muscular Atrophy. N Engl J Med 377, 1713–1722 (2017). [PubMed: 29091557]
76. Gibbons GS et al. , Conformation-selective tau monoclonal antibodies inhibit tau pathology in primary neurons and a mouse model of Alzheimer's disease. Mol Neurodegener 15, 64 (2020). [PubMed: 33148293]
77. Tang J et al. , Critical role for Daxx in regulating Mdm2. Nat Cell Biol 8, 855–862 (2006). [PubMed: 16845383]
78. Huang L et al. , DAXX represents a new type of protein-folding enabler. Nature 597, 132–137 (2021). [PubMed: 34408321]
79. Li W, Lee VM, Characterization of two VQIXXK motifs for tau fibrillization in vitro. Biochemistry 45, 15692–15701 (2006). [PubMed: 17176091]
80. Harischandra DS et al. , Manganese promotes the aggregation and prion-like cell-to-cell exosomal transmission of alpha-synuclein. Sci Signal 12, (2019).
81. Guo JL, Lee VM, Neurofibrillary tangle-like tau pathology induced by synthetic tau fibrils in primary neurons over-expressing mutant tau. FEBS Lett 587, 717–723 (2013). [PubMed: 23395797]
82. Lock M et al. , Rapid, simple, and versatile manufacturing of recombinant adeno-associated viral vectors at scale. Hum Gene Ther 21, 1259–1271 (2010). [PubMed: 20497038]

83. Kai H et al. , Enhanced antigen retrieval of amyloid beta immunohistochemistry: re-evaluation of amyloid beta pathology in Alzheimer disease and its mouse model. J Histochem Cytochem 60, 761–769 (2012). [PubMed: 22821668]

84. Gordon R et al. , Prokineticin-2 upregulation during neuronal injury mediates a compensatory protective response against dopaminergic neuronal degeneration. Nat Commun 7, 12932 (2016). [PubMed: 27703142]

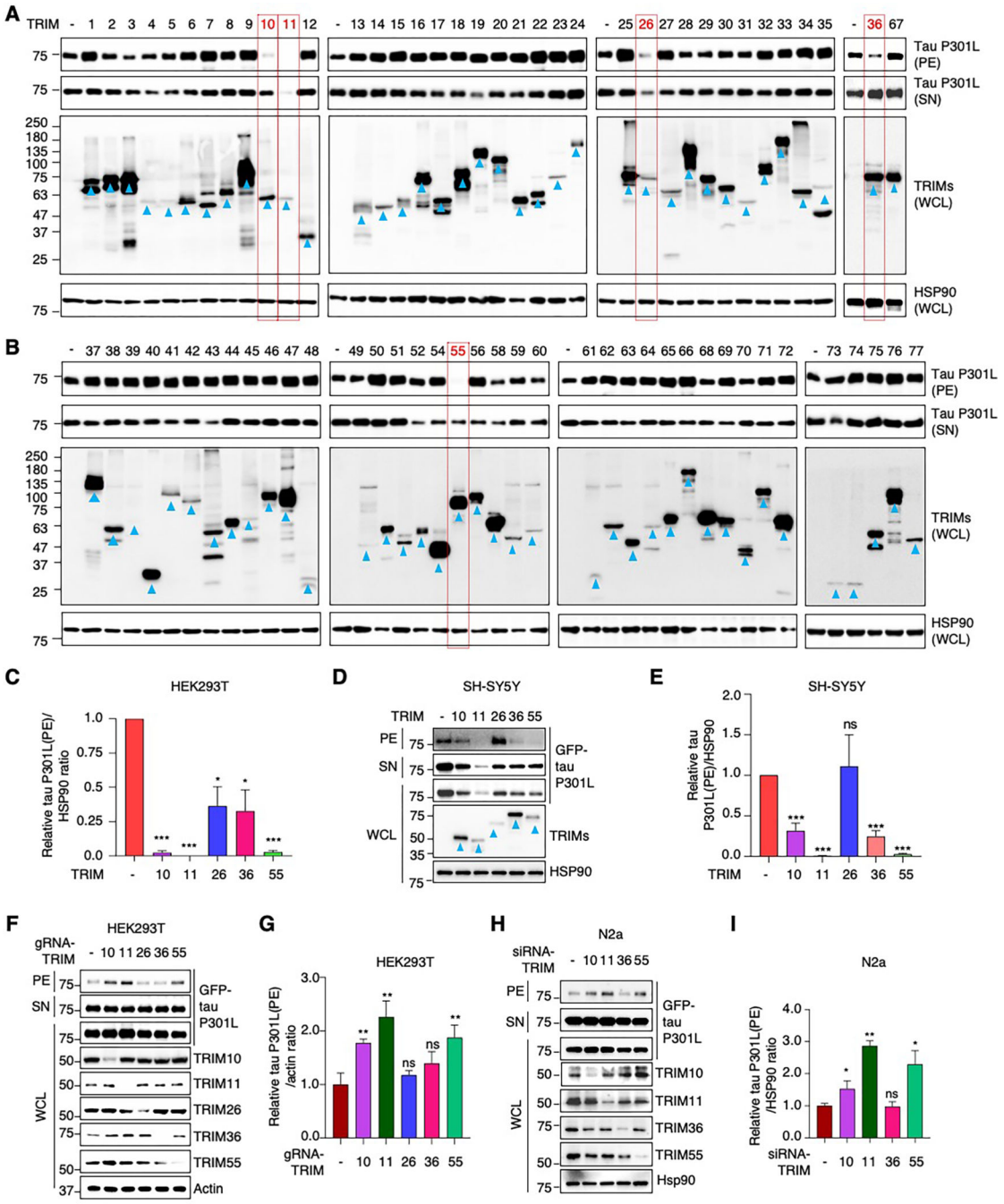

Fig. 1. Screening of TRIM proteins

(**A** to **E**) Immunoblot of HEK293T (A and B) or SH-SY5Y (D) cells co-transfected with GFP-tau P301L and control vector (−) or the indicated TRIMs, and quantification of relative GFP-tau P301L(PE)/HSP90 ratios (C and E). SN, NP-40-soluble supernatant. PE, NP-40-insoluble pellets. WCL, whole cell lysates. The expected full-length TRIM bands are indicated by blue arrowheads. In (A) and (B), TRIM proteins that substantially reduced insoluble GFP-tau P301L species are labeled in red boxes.

(**F** to **I**) Immunoblot of TRIM-knockout HEK293T (F) or TRIM-knockdown N2a (H) cells transfected with GFP-tau P301L, and quantification of relative GFP-tau P301L(PE)/HSP90 ratios (G and I).

Data are mean ± SD, n = 3. *$P < 0.05$, **$P < 0.01$, ***$P < 0.001$; unpaired Student's t test.

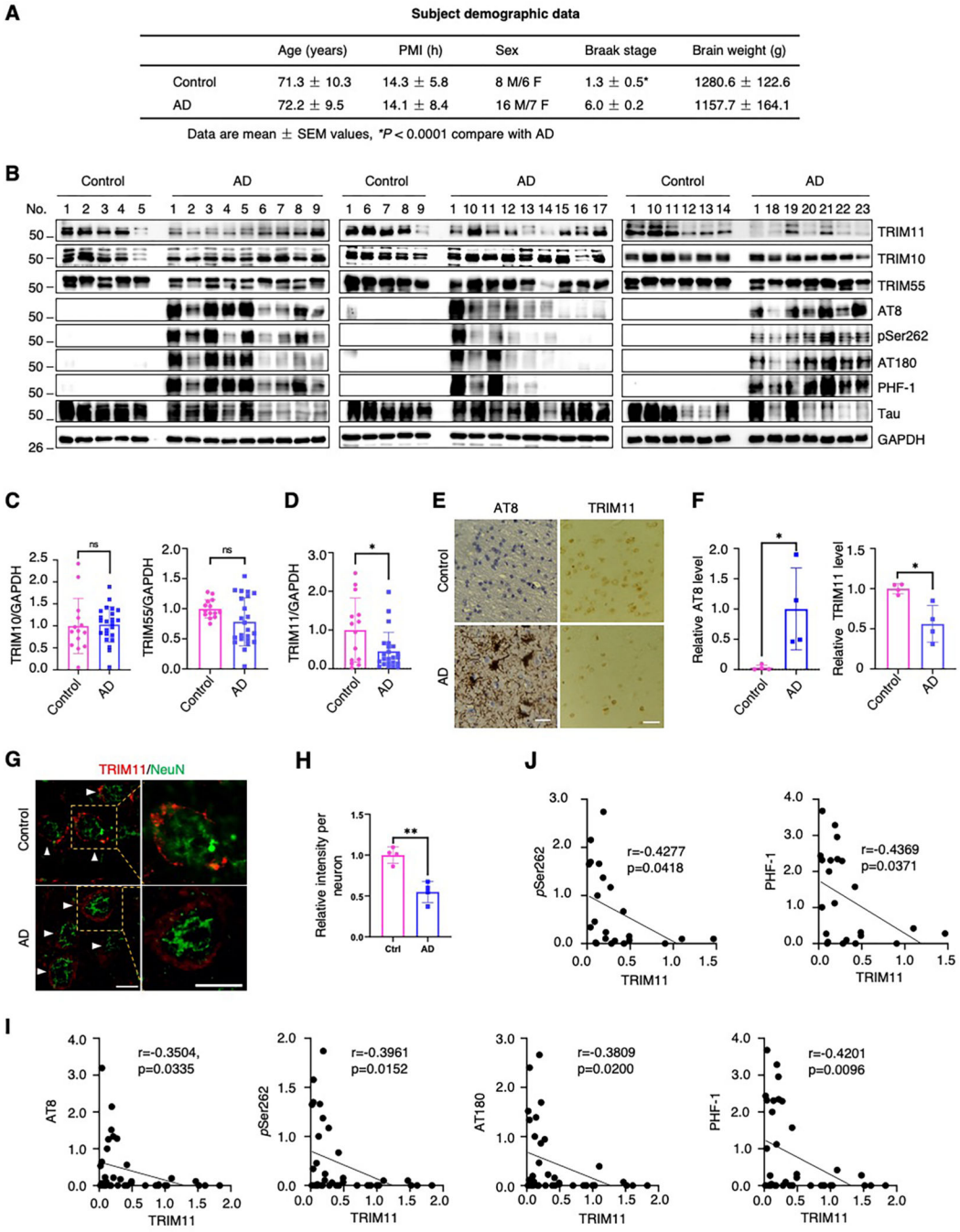

Fig. 2. Downregulation of TRIM11 in sporadic AD brains

(**A**) Summary of demographic data of control and AD subjects used in this study. Information on individual subjects is provided in Table S2.

(**B** to **D**) Immunoblot of postmortem frontal cortex gray matters from 14 control and 23 AD individuals (B), and relative levels of TRIM10 and TRIM55 (C), and TRIM11 (D) in AD vs. control samples. The #1 control and #1 AD samples were used in each blot as standards. p-Tau species were modified at residues S202/T205 (reactive to AT8), Ser262, T231 (reactive to AT180), and S396/S404 (reactive to PHF-1).

(**E** and **F**) Representative IHC images of TRIM11 and AT8-reactive p-tau in frontal cortices (E; scale bar, 50 μm), and quantification of TRIM11 and AT8 signals (F; mean ± SD, n = 4).
(**G** and **H**) Representative IF images of TRIM11 and NeuN in frontal cortices of control and AD samples (G; scale bar, 10 μm), and quantification of TRIM11 signal normalized to numbers of neurons (H; mean ± SD, n = 4). Individual neurons are indicated by white arrows.
(**I** and **J**) Negative correlation between levels of TRIM11 and different p-tau species among AD and control tissues (I) or AD tissues only (J). The *r* and *p* values of Pearson correlation coefficient are shown.
**P* < 0.05; ***P* < 0.01; ns, not significant; unpaired Student's t test.

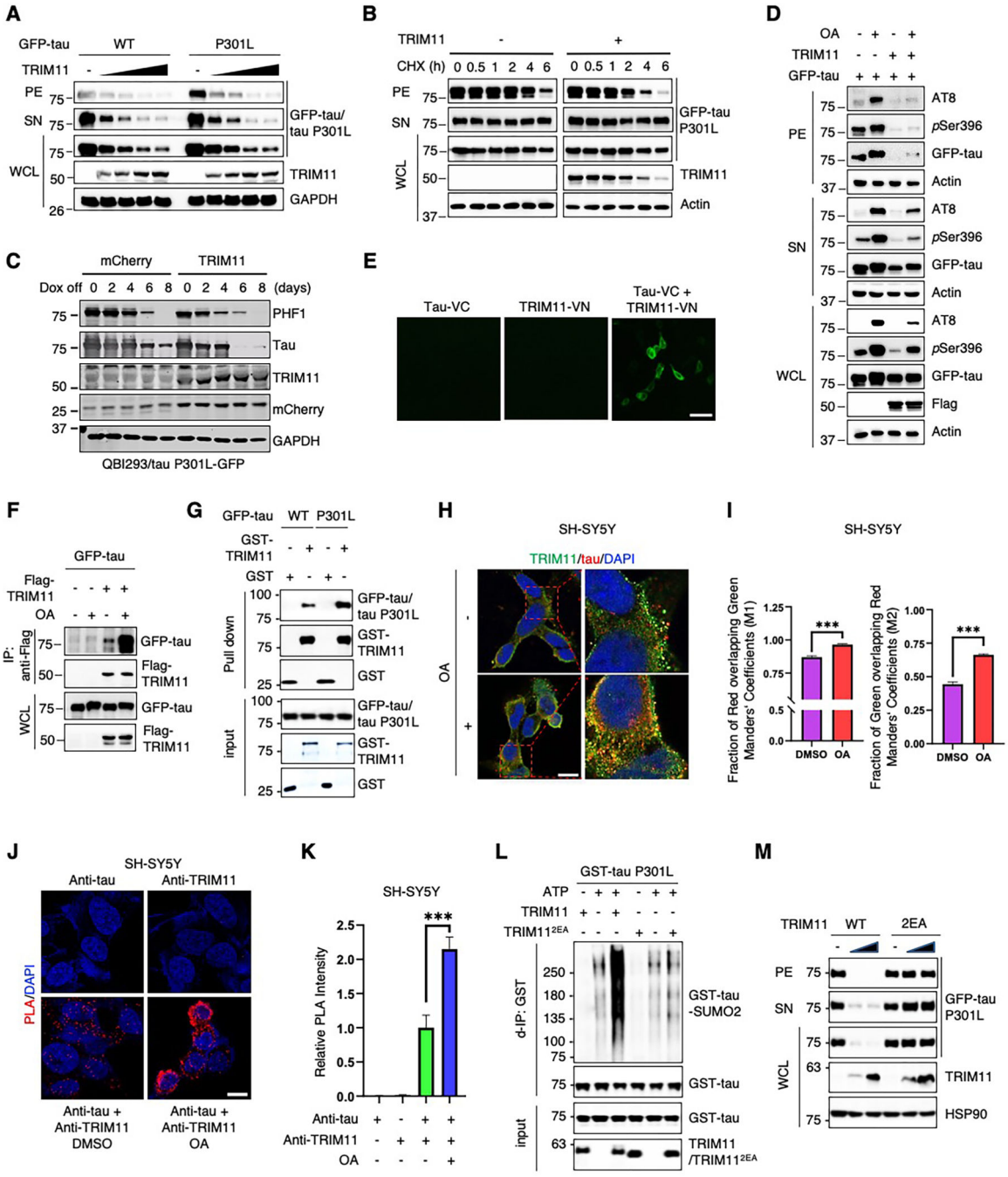

Fig. 3. TRIM11 binds to tau and targets it for proteasomal degradation

(**A**) Levels of sarkosyl-insoluble (PE) and -soluble (SN) tau and tau P301L in HEK293T cells in the absence or presence of TRIM11.

(**B**) Turnover of GFP-tau P301L in HEK293T cells in the absence or presence of TRIM11. The tau blots on the left and the right sides were exposed for different times for better comparison.

(**C**) Turnover of tau and p-tau in QBI293/tau P301L-GFP cells stably expressing mCherry or mCherry plus TRIM11.

(**D**) Levels of GFP-tau and p-GFP-tau when expressed alone or together with TRIM11 in HEK293T cells, which were subsequently treated with or without OA (100 nM). To achieve comparable levels of GFP-tau, the amount of GFP-tau plasmid was increased when expressed together with TRIM11 (fig. S5E).

(**E**) BiFC assay of TRIM11-VN and tau-VC interaction in HEK293T cells (scale bar, 100 μm).

(**F**) Interaction of Flag-TRIM11 and GFP-tau in HEK293T cells treated with or without OA.

(**G**) Interaction of GST-TRIM11 with 6×His-GFP-tau and 6×His-GFP-tau P301L in vitro.

(**H** and **I**) Localization of endogenous TRIM11 and tau in SH-SY5Y cells treated with or without OA (H; scale bar, 10 μm), and Manders' co-localization coefficient (I).

(**J** and **K**) PLA of endogenous TRIM11-tau interaction in SH-SY5Y cells treated with or without OA (J; scale bar, 10 μm) and quantification of PLA signals (K).

(**L**) SUMOylation of purified GST-tau P301L protein in the presence of TRIM11 or $TRIM11^{2EA}$.

(**M**) Levels of GFP-tau P301L in HEK293T cells in the presence of TRIM11 or $TRIM11^{2EA}$.

Data are mean ± SEM, n = 3. ***$P < 0.001$, unpaired Student's t test.

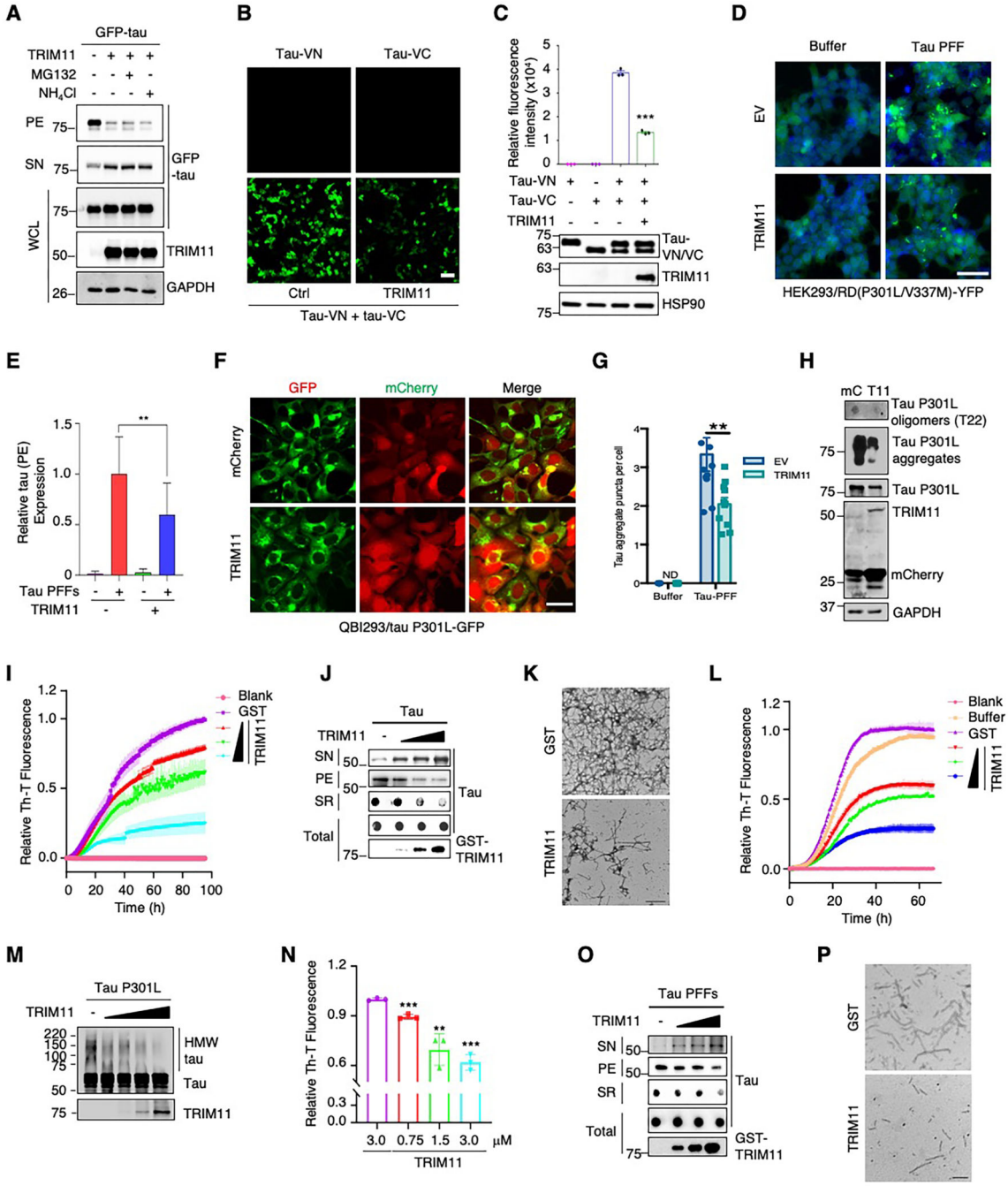

Fig. 4. TRIM11 is a molecular chaperone and a disaggregase for tau, increasing its solubility.

(**A**) Effect of TRIM on GFP-tau levels in HEK293T cells treated as indicated. Different amounts of GFP-tau plasmid were used when transfected with or without TRIM11 to achieve comparable total levels.

(**B** and **C**) BiFC assay for tau-VN and tau-VC interaction with or without TRIM11. Shown are representative cell image (B; scale bar, 100 μm), relative fluorescence signal (C, top), and protein expression (C, bottom).

(**D** and **E**) Representative image (D; scale bar, 100 μm) and quantification (E) of tau inclusions in HEK293/RD(LM)-YFP cells transfected with or without TRIM11 and treated as indicated.

(**F** to **H**) Representative image (F; scale bar, 50 μm) and quantification (G) of tau inclusions in, and insoluble tau species in lysates from (H), QBI293/tau P301L-GFP cells stably expressing mCherry, or mCherry plus TRIM11, and treated without (G) or with (F to H) PFFs.

(**I** to **K**) ThT binding (I), sedimentation (J), and EM (K; scale bar, 500 nm) analyses of fibril formation by tau-441 (10 μM) in the presence of GST (1 μM) or GST-TRIM11 (0.25, 0.5, or 1 μM).

(**L** and **M**) Formation of fibrils (L) and high molecular weight species (M) by tau-441 P301L incubated with GST (1 μM) or GST-TRIM11 (0.25, 0.5, or 1 μM).

(N to **P)** ThT-binding (N), sedimentation (O), and EM (P; scale bar, 200 nm) analyses of tau-441 fibrils treated with GST or GST-TRIM11 at indicated concentrations (N and O) or 3.0 μM (P).

Data are mean ± SD, n = 3 for (C), (E), and (N), and 8 for (G). $^{**}P < 0.01$, $^{***}P < 0.001$; unpaired Student's t test.

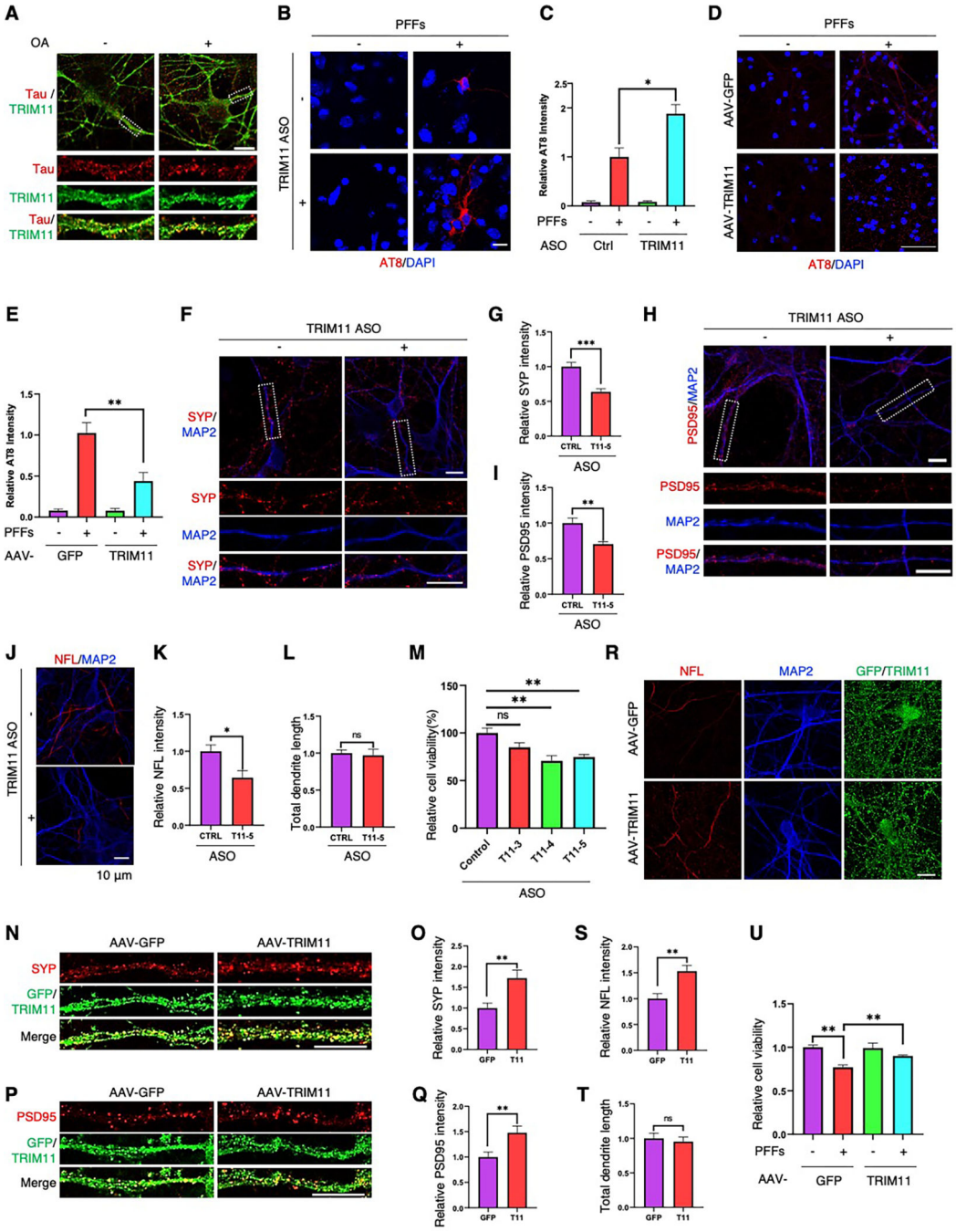

Fig. 5. TRIM11 maintains neural integrity and connectivity

(**A**) Co-localization of endogenous TRIM11 and tau in wild-type cortical neurons. Scale bar, 10 μm.

(**B** to **E**) Images (B and D) and quantification (C and E) of intracellular AT8-reactive tau aggregates in PS19 cortical neurons that were transduced with control or TRIM11 ASO (B and C), or with AAV9-GFP or AAV9-TRIM11 (D and E), and treated with myc-K18/P301L PFFs. Scale bar, 10 μm in (B) and 50 μm in (D).

(**F** to **I**) Images (F and H; scale bar, 10 μm) and quantifications (G and I) of SYP- or PSD-reactive puncta in wild-type cortical neurons treated with control or TRIM11 ASO.
(**J** to **L**) Images of NFL and MAP2 staining (J; scale bar, 10 μm), and relative intensity of NFL staining (K) or length of MAP2-stained dendrites (L) normalized to neuronal cell number, in wild-type cortical neurons treated with control or TRIM11 ASO.
(**M**) Viability of wild-type cortical neurons treated with control ASO or the indicated TRIM11 ASOs.
(**N** to **Q**) Images (N and P; scale bar, 10 μm) and quantifications (O and Q) of SYP- or PSD95-reactive puncta in wild-type cortical neurons transduced with AAV9-GFP or AAV9-TRIM11.
(**R** to **T**) Images of NFL, MAP2, and GFP/TRIM11 staining (R; scale bar, 10 μm), and quantifications of relatively NFL and MAP2 intensity normalized to neuronal cell number (S and T; mean ± SEM), in wild-type cortical neurons transduced with AAV9-GFP or AAV9-TRIM11.
(**U**) Viability of wild-type cortical neurons transduced with AAV9-GFP or AAV9-TRIM11 and treated with or without tau PFFs.
Data are mean ± SEM, n = 6 for (M) and 3 for the rest. *$P < 0.05$, **$P < 0.01$, ***$P < 0.001$, ns, not significant; unpaired Student's t test.

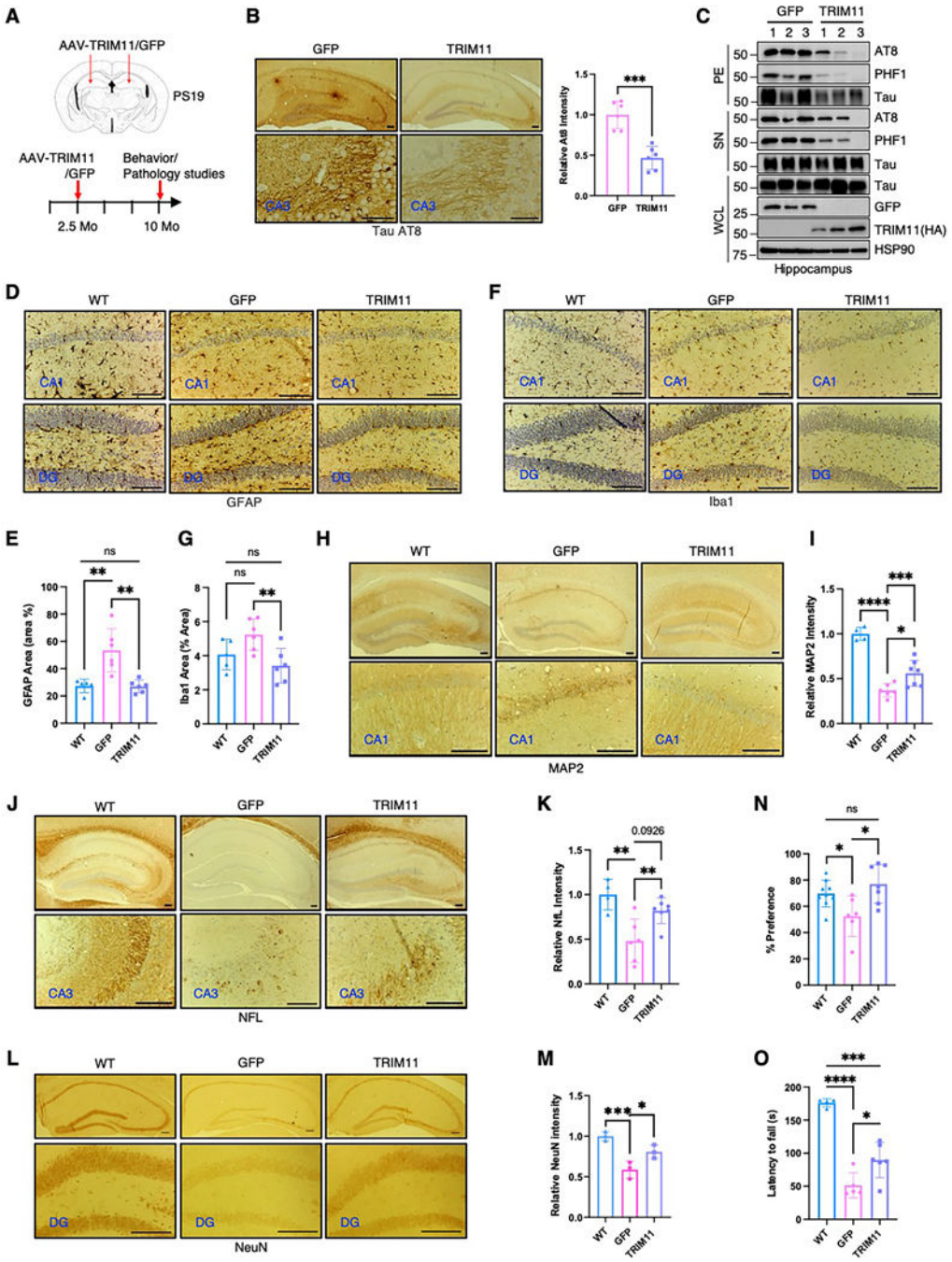

Fig. 6. TRIM11 protects against tau pathology and cognitive/behavioral impairments in PS19 mice

(**A**) Schematic representation of the study.

(**B**) Representative IHC images of the hippocampus stained with AT8 (left; scale bar: 0.2 mm) and relative AT8 intensity (right; mean ± SD, n = 6 mice).

(**C**) Immunoblot of total tau and p-tau species in the hippocampus. Each lane represents a single mouse.

(**D** to **M**) Representative IHC images and quantification of GFAP (D and E), Iba1 (F and G), MAP2 (H and I), NFL (J and K), and NeuN (L and M) staining. Scale bar: 0.2 mm. Data are mean ± SD, n = 3 to 7 mice. DG, dentate gyrus.

(**N** and **O**) Preference for the novel in ORT (N) and latency to fall in wire hang test (O) (mean ± SD, n = 4 to 7 mice).

*$P < 0.05$; **$P < 0.01$; ***$P < 0.001$; ****$P < 0.0001$, ns, not significant; unpaired Student's t test.

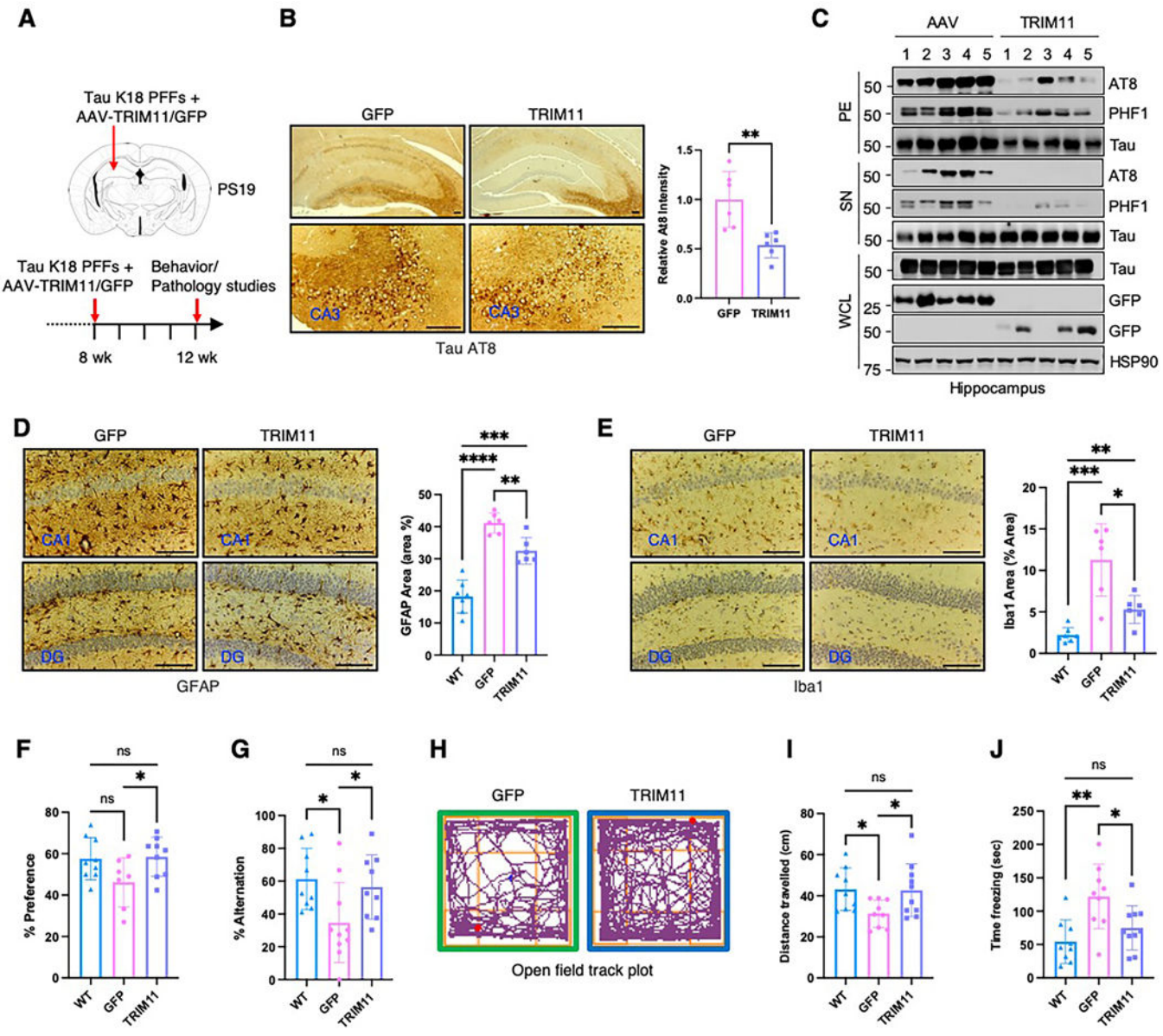

Fig. 7. TRIM11 ameliorates PFFs-accelerated tau pathology and cognitive/behavioral impairments in PS19 mice

(**A**) Schematic representation of the study.

(**B, D**, and **E**) IHC staining with AT8 (B) or anti-GFAP (D) or -Iba1 (F) antibody of the hippocampus (left), and quantification of AT8 (B), GFAP (D), or Iba1 (F) immunoreactivity (right; mean ± SD, n = 5 to 6 mice).

(**C**) Immunoblot of tau and p-tau species in the hippocampus. Each lane represents a single mouse.

(**F**) Preference for the novel subject in ORT (mean ± SD, n = 7 or 9 mice).

(**G** to **J**) Alternation in Y-maze (G), and travel distance (H and I) and freezing time (J) in the open field maze (mean ± SD, n = 9 or 10 mice).

**P* < 0.05; ***P* < 0.01; ****P* < 0.005; ns, not significant; unpaired Student's t test.

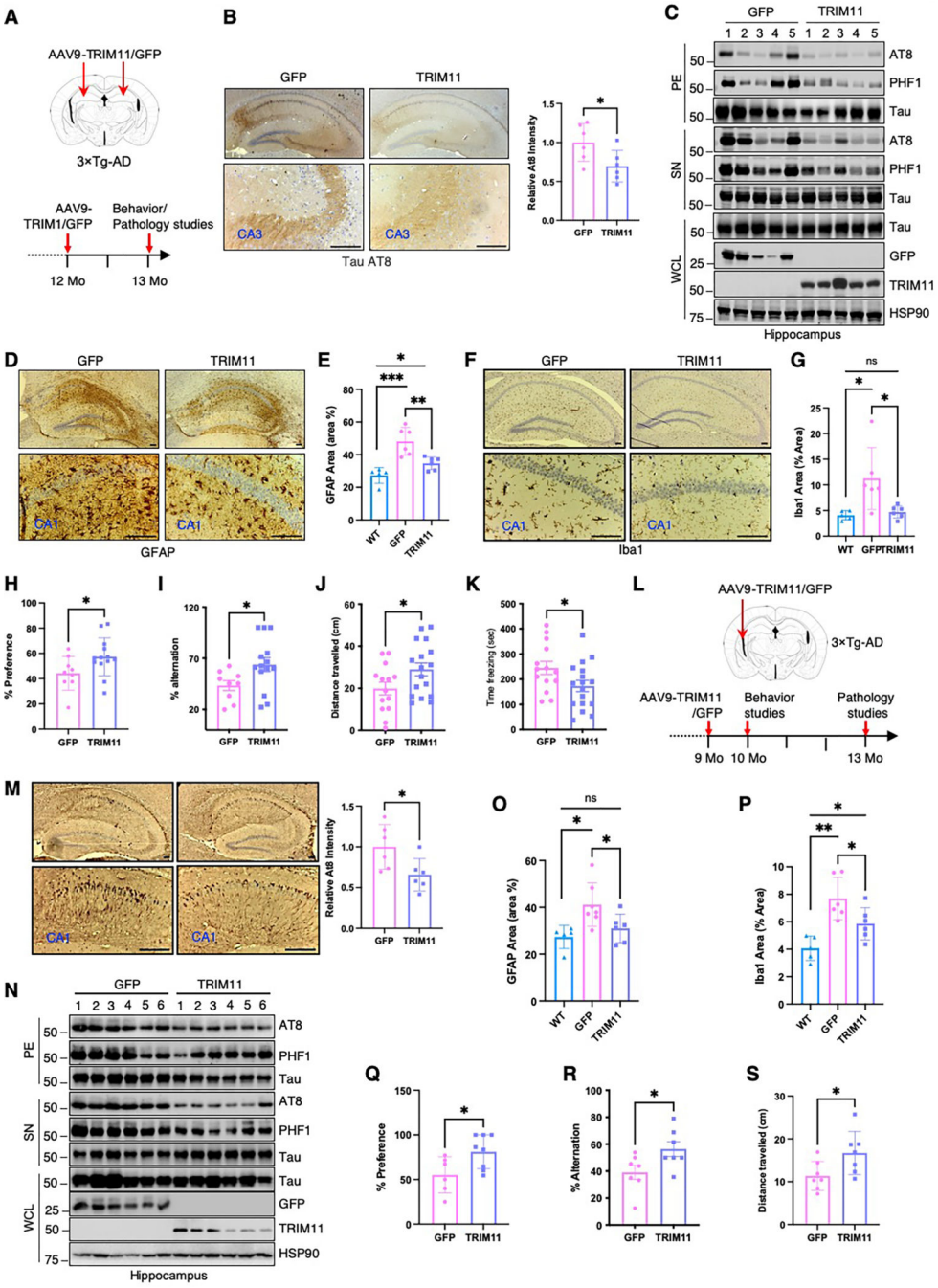

Fig. 8. TRIM11 ameliorates tau pathology and cognitive deficits of 3×Tg-AD mice

(**A** and **L**) Schematic representation of bilateral IP (A) and unilateral ICV (L) injection of 3×Tg-AD mice.

(**B** and **M**) AT8 staining of hippocampi from mice injected with the indicated AAV vector via IP (B) or ICV (M) (left; scale bar, 0.2 mm) and quantification of AT8 signal (right; means ± SD, n = 6 mice).

(**C** and **N**) Immunoblot of tau and p-tau species in the hippocampus of mice injected with indicated AAV vectors via IP (C) or ICV (L). Each lane represents a single mouse

(**D** to **G**, **O**, and **P**) Representative IHC images (D and E; scale bar, 0.2 mm) and quantification of GFAP- or Iba1-immunoreactivity (E, G, O, and P; means ± SD, n = 5 to 6 mice) of the hippocampus of mice injected with AAV vectors via IP (D to G) or ICV (O and P).

(**H**, **I**, **Q**, and **R**) Preference for the novel object in ORT (H and Q) and alternation in Y-maze(I and R) by mice injected with AAV vectors via IP (H and I) or ICV (Q and R). Data are means ± SD, n = 6 to 14 mice.

(**J**, **K**, and **S**) Travel distance (J and S) and freezing time (K) of mice injected with AAVs in the hippocampus (J and K) or CSF (S). Data are means ± SD, n = 7 to 17 mice.

* $P < 0.05$; ** $P < 0.01$; *** $P < 0.005$; ns, not significant; unpaired Student's t test.